

Received: 02.11.2022

Accepted: 18.04.2023

Research Article

**Could *Zingiber officinale* plant be effective against Omicron BA.2.75 of SARS-CoV-2?**

Handan SARAC, Ahmet DEMİRBAŞ, Burak TÜZÜN<sup>1</sup>

Plant and Animal Production Department, Technical Sciences Vocational School of Sivas, Sivas  
Cumhuriyet University, Sivas, Turkey

**Abstract:** *Zingiber officinale* plant was examined in this study. The chemicals found in this plant were identified using the GC-MS method. The activities of the determined chemical molecules against the SARS-CoV-2 Omicron variant were compared. We focused to determine whether *Zingiber officinale* plant would be an inhibitor against Omicron of SARS-CoV-2 in silico. As a result of theoretical calculations, *Zingiber officinale* plant was found to contain many chemicals as a result of GC-MS analysis. These chemicals were detected one by one and their activity values were calculated for the SARS-CoV-2 virus. As a result, molecules with high activity were detected. ADME/T properties were investigated in order to examine the drug properties of molecules with high activity. According to ADME/T results, these five molecules examined are suitable for use in human metabolism as drug molecules.

**Keywords:** *Zingiber officinale*, SARS-CoV-2, Omicron, Molecular docking, ADME/T

## 1. Introduction

Coronavirus disease 2019 (COVID-19) is a deadly disease caused by a new coronavirus (SARS-CoV-2) that spreads rapidly and poses a global threat. Indeed, it was declared a pandemic disease in 2020 by the World Health Organization (WHO) [1-3]. It has been determined that the most common mode of transmission of COVID-19, which is responsible for the 21st century pandemic, is through respiratory droplets or nasal secretions [3,4]. The disease spreads rapidly through the sneezing and coughing fluid of an infected person [2]. It is also known to have features similar to severe acute respiratory syndrome (SARS) [4,5]. Most cases of COVID-19 show flu-like symptoms, and common clinical symptoms include fever, dry cough, common cold, shortness of breath, acute respiratory distress syndrome (ARDS), kidney failure, and multiple organ failure [1,2,4]. The incubation period of the disease ranges from 3 to 14 days [3]. The threat to public health has reached serious levels, especially due to the high contagiousness of atypical pneumonia caused by it [1,4]. There is no anti-virus drug that can be used for corona virus [2,4]. Therefore, in addition to vaccine

development studies, therapeutic alternatives are sought to prevent the COVID-19 pandemic. In this context, a possible anti-viral drug molecule or molecules for corona virus can be discovered in line with traditional and ethnobotanical knowledge [2]. Knowing that plants have healing effects goes back to ancient times [6]. Since ancient times, plants have been used by humans as medicine for the treatment of various diseases [7]. Today, the use of herbal medicines for treatment is of great interest [4]. There are various phytochemical substances obtained from plants in the composition of many drugs available on the market [6], and herbal drugs are considered to be the most effective and safe way to protect or treat health [4]. Therefore, more scientific studies are needed to prove the safety and clinical effects of traditional herbal medicines [3]. Ginger (*Zingiber officinale*) is a perennial rhizome plant belonging to the *Zingiberaceae* family, native to East and South Asia [6,8,9]. It is cultivated for commercial purposes in various countries such as India, China, Australia, South East Asia, Mexico [6,10]. In addition to being widely used as a spice and flavoring agent, it has also been used as a medicine in the treatment of various diseases due to

<sup>1</sup> Corresponding Authors

e-mail: theburaktuzun@yahoo.com; btuzun@cumhuriyet.edu.tr

its medicinal effects since ancient times [6,7,10,11]. It has an important place especially in traditional Chinese and Indian medicine [11]. Its rhizomes are used to alleviate or treat ailments such as colds, bronchitis, fever, headache, cough, colic, indigestion and nausea [6,8,9]. It is known to be effective against pathogens, especially in the treatment of respiratory diseases [12]. It has a rich chemical content in terms of phenolic compounds, terpenes, polysaccharides, lipids and organic acids [9]. Its medicinal properties are due to the phenolic compounds it contains [5,9]. Studies so far show that ginger has multiple biological activities (such

as antioxidant, anti-inflammatory, antimicrobial, anticancer) [7,8,9,13]. Recently, it has been tried to determine the effects of ginger on COVID-19. In studies conducted so far, it has been determined that some medicinal plants, especially ginger, have promising potential in preventing or treating the COVID-19 epidemic. For example, by the National Traditional Administration of Chinese Medicine (NATCM), 90% of COVID-19 patients using an herbal medicine called Qing Fei Pai Du Tang (a mixture of ginger, belamcayenne, dioscoreae, glycyrrhiza glabra, etc.) reactions have been reported [4].

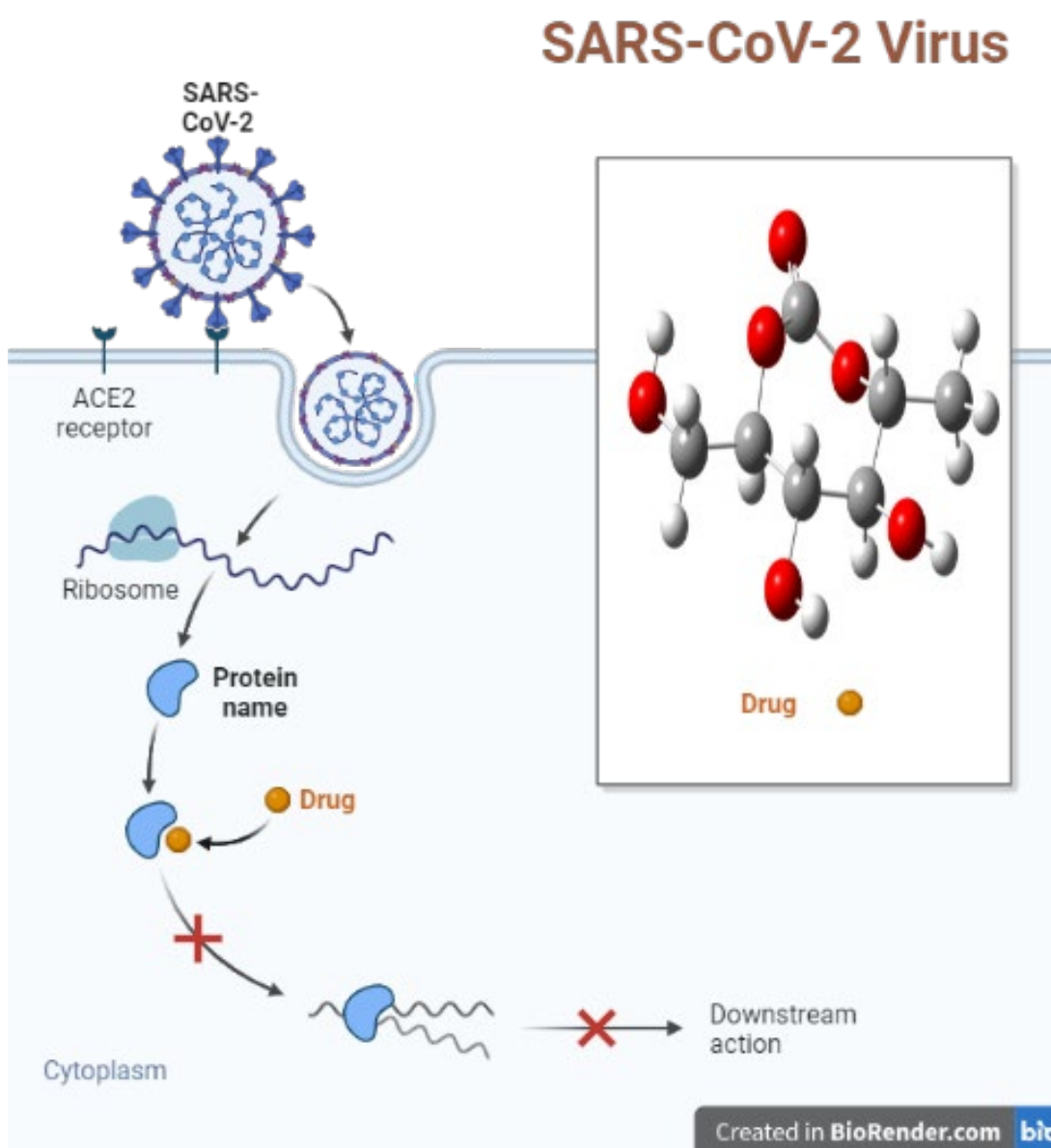


**Figure 1.** Demonstration of SARS-CoV-2 virus entry into the cell

When the movements of the SARS-CoV-2 virus in human metabolism are examined, it is seen in detail in Figure 1 that this virus enters the cell by attaching to the angiotensin-converting enzyme 2 (ACE 2) receptor site when it enters the cell. With the drugs developed, the movements of this virus in the cell are restricted and inhibited. When the movements of the SARS-CoV-2 virus in human metabolism are examined, it is seen in detail in Figure 1 that this virus enters the cell by attaching to the ACE 2 receptor site when it enters the cell. With the drugs developed, the movements of this virus in the cell are restricted and inhibited. There are many drug molecules developed and used [14-17]. These drugs are put on the market after they are approved by the FDA (U.S. Food and Drug Administration) in the USA.

In one of the molecular docking studies, some phytochemicals of the ginger plant were found to have spike protein (S protein) in SARS-CoV-2, which is involved in the recognition of the host cell and virus-host membrane fusion, and angiotensin-converting enzyme 2 (ACE), which is a strong SARS-CoV receptor-2 [12]. In another Docking study, it was determined that 9 out of 42 phytochemical molecules obtained from *Z. officinale* were most likely against the main protease enzyme of COVID-19 and could be potential anti-virals [5].

In this study, extract chemicals from the *Zingiber officinale* plant were used to develop effective inhibitor candidates for the prevention of Omicron variant BA.2.75 of SARS-CoV-2 virus. In this study, crystal structure of SARS-CoV-2 S Omicron Variant Spike protein (PDB ID: 7QO7) [18], crystal structure of SARS-CoV-2 omicron Variant with human ACE2 protein (PDB ID: 7U0N) [19], and crystal structure of SARS-CoV-2 Omicron Variant proteins (PDB ID: 7WRV) [20] were used. The activities of the molecules in the extract were compared against these proteins. These comparison results were compared with FDA-approved drugs used for SARS-CoV-2 virus.

## 2. Computational Method

### 2.1. Obtaining the extract

Supply of the plant: Within the scope of the study, fresh rhizomes of the ginger plant were used as plant material. Fresh rhizomes of the plant were purchased from the local market.

### 2.2. Ethanol extraction

Plant rhizomes brought to the laboratory environment were washed with distilled water and dried with a towel. Then, the bark of the rhizomes was peeled off and cut into small pieces with the

help of a household rondo. 50 g of the plant material, which was turned into small particles, was weighed, 500 mL of 80% ethanol (1:10) was added, and macerated in an electronic shaker at room temperature ( $25\pm 2^\circ\text{C}$ ) for 24 hours at 150 rpm. After maceration, Whatman No. Filtering was done twice with the help of 1 filter paper. The solvent removal process from the obtained filtrate was carried out at  $40^\circ\text{C}$  in a rotary evaporator (Büchi). The remaining dry extract was stored in a brown glass bottle at  $+4^\circ\text{C}$  for a short time.

### 2.3. GC-MS Analysis

GC-MS analysis of the ethanol extract obtained from the rhizomes of the ginger plant was performed in Sivas Cumhuriyet University, Advanced Technology Research and Development Center as a service procurement. In the analysis, Shimadzu GCMS-QP2010 Ultra device, Rxi-5ms (30mx0.25x0.25) Capillary column and Helium (1.5 mL/min) as carrier gas were used. The injection temperature was set at  $280^\circ\text{C}$ , the injection volume was  $1\mu\text{L}$ , and the pressure was set as 100 kPa. Injection mode is splitless, MS mode is Scan, 35-550 m/z. The ion source temperature was used as  $200^\circ\text{C}$ . The oven temperature program was set from  $60^\circ\text{C}$  to  $320^\circ\text{C}$  with an increase of  $5^\circ\text{C}/\text{min}$  and the total time was 57 minutes.

### 2.4. Theoretical calculations

To compare a molecule's biological activity to a biological substance, molecular docking calculations are used. For the computations of molecular docking, Schrödinger [21] employed the Maestro Molecular modeling platform (version 12.8) program. Numerous processes go into calculations. Every stage is carried out uniquely. The first phase involved using the protein preparation module [22], the second involved using the LigPrep module [23], and the third involved using the Glide ligand docking module [24]. All computations were performed using the OPLS4 method. In order to assess the potential therapeutic value of the investigated compounds, an ADME/T analysis (absorption, distribution, metabolism, excretion, and toxicity) will be carried out. The Qik-prop module [25] of the Schrödinger software was used to predict the effects and reactions of molecules in human metabolism.

## 3. Results and discussion

GC-MS analysis was performed to determine the chemical in the ethanol extract obtained from the *Zingiber officinale* plant. As a result of this analysis, 109 different chemicals were found in this extract. Most of the 109 chemicals were found to be

in trace amounts. As a result, the chemicals found as a result of the GC-MS analysis are given in Table 1.

**Table 1.** Chemicals found in the ethanol extract of the *Zingiber officinale* plant

Molecule no	Molecule name	RT
1	(3R,5S)-1-(4-Hydroxy-3-methoxyphenyl)decane-3,5-diyl diacetate	42.030
2	(E)-1-(4-Hydroxy-3-methoxyphenyl)dec-3-en-5-one	36.886
3	(E)-1-(4-Hydroxy-3-methoxyphenyl)dodec-3-en-5-one	37.195
4	(E)-1-(4-Hydroxy-3-methoxyphenyl)hexadec-4-en-3-one	42.849
5	(E)-1-(4-Hydroxy-3-methoxyphenyl)tetradec-3-en-5-one	41.209
6	(E)-1,7-bis(4-Hydroxy-3-methoxyphenyl)hept-4-en-3-one	37.871
7	(S)-1-(4-Hydroxy-3-methoxyphenyl)-3-oxodecan-5-yl acetate	38.164
8	(Z)-4,6-Dioxohept-2-enoic acid, di-TMS	13.470
9	Beta.-Sitosterol	54.357
10	Beta.-Sitosterol, TMS derivative	54.886
11	Gamma.-Sitosterol	54.357
12	(2-(2-Ethoxyethoxy)ethoxy)acetic acid, TMS derivative	8.571
13	1-(2,4-Dihydroxyphenyl)-2-(4-methoxy-3-nitrophenyl)ethanone	38.589
14	1-(3,4-Dimethoxyphenyl)decane-3,5-diyl diacetate	42.386
15	1-(4-Hydroxy-3-methoxyphenyl)dec-4-en-3-one	37.871
16	1-(4-Hydroxy-3-methoxyphenyl)dodec-4-en-3-one	42.849
17	1-(4-Hydroxy-3-methoxyphenyl)octane-3,5-diyl diacetate	42.030
18	1-(4-Hydroxy-3-methoxyphenyl)tetradec-4-en-3-one	45.005
19	1,3,9,11,2,10-Parazabol, 2,2,10,10-tetraethyl-	19.734
20	1,3-Dioxolane, 2-methyl-	5.819
21	1,4-Dioxan-2-ol, TMS derivative	26.191
22	1,5-Anhydro-d-mannitol	20.195
23	1,5-Anhydrohexitol, 4TMS derivative	28.580
24	13-Docosenamide, (Z)-	45.931
25	16-Methyl-heptadecanecarboxylic acid trimethylsilyl ester	37.195
26	1-Methoxy-5-trimethylsilyloxyhexane	9.883
27	1-Monopalmitin, 2TMS derivative	43.160
28	1-Propanol, TMS derivative	8.571
29	2,2,18,18-Tetramethyl-3,6,10,13,17-Pentaoxa-2,18-Disilaneonadecane	27.439
30	2,2,5,9,9-Pentamethyl-3,8-Dioxa-2,9-Disiladecane	26.191
31	2,2'-Ureylenebis(ethyl 3,3,3-trifluorolactate)	6.286
32	2,3-Dihydro-Benzofuran	13.665
33	2,3-Dihydro-3,5-dihydroxy-6-methyl-4H-pyran-4-one	11.592
34	2,3-Dimethyl-3-pentanol, TMS derivative	27.021
35	2,5-Monomethylene-l-rhamnitol	20.304
36	2-Hydroxyisocaproic acid, trimethylsilyl ester	21.542
37	2-Ketohexanoic acid, trimethylsilyl ester	21.542
38	2-Methyl-1,4-bis(trimethylsilyloxy)butane	26.191
39	2-Methylcyclohexanol, (Z)-, TMS derivative	12.676
40	2-Mono-isobutyryn, 2TMS derivative	24.969
41	2-Mono-isobutyryn, bis(trimethylsilyl)-	27.021
42	3,6-Dioxaoctanedioic acid, TMS derivative	9.883
43	3,7,11,15,18-Pentaoxa-2,19-disilaicosane, 2,2,19,19-tetramethyl-	27.439
44	3,8-dioxa-2,9-disiladecan-5-one, 2,2,6,6,9,9-hexamethyl-	27.021

45	3-Methoxy-N-(trifluoroacetyl)-O-(trimethylsilyl)tyrosine, trimethylsilyl ester	38.589
46	3-Methyl-2-ketobutyric acid tbdms	21.542
47	3-Penten-2-one, 4-(2,2,6-trimethyl-7-oxabicyclo(4.1.0)hept-1-yl)-, (E)-	41.209
48	4-Decen-3-one, 1-(4-hydroxy-3-methoxyphenyl)-, (E)-	38.164
49	4H-Pyran-4-one, 2,3-dihydro-3,5-dihydroxy-6-methyl-	11.592
50	4-Methoxymandelic acid, ethyl ester, TMS	39.029
51	4-Octanol, TMS derivative	27.021
52	4-Tetradecen-3-one, 1-(4-hydroxy-3-methoxyphenyl)-, (E)-	45.005
53	5-Hydroxy-1-(4-hydroxy-3-methoxyphenyl)dodecan-3-one	42.849
54	5-Hydroxymethyl-2,2,5-trimethyl-1,3-dioxane, TMS derivative	24.969
55	6-Methoxy-2-hexanol, TMS derivative	9.883
56	6-Nonenamide, N-((3-methoxy-4-((trimethylsilyl)oxy)phenyl)methyl)-8-methyl-, (E)-	39.029
57	9,12-Octadecadienoic acid (Z,Z)-	35.141
58	9,12-Octadecadienoic acid (Z,Z)-, TMS derivative	36.642
59	9-Octadecenamide	45.931
60	Acetin, bis-1,3-trimethylsilyl ether	24.969
61	Alpha.-D-Mannopyranoside, methyl 2,3-bis-O-(trimethylsilyl)-, cyclic butylboronate	31.747
62	Arabinonic acid, 2,3,4-tris-O-(trimethylsilyl)-, lactone, D-	29.112
63	Benzyl-diethyl-(2,6-xylyl-carbamoylmethyl)-ammonium benzoate	42.179
64	Beta.-D-Xylopyranose, 4TMS derivative	31.277
65	Butanoic acid, 4-((trimethylsilyl)oxy)-, trimethylsilyl ester	21.542
66	Butoxytriglycol, TMS derivative	26.326
67	Butyric Acid, TMS derivative	25.499
68	Capsaicin	41.209
69	Capsaicin, TMS derivative	39.029
70	Cyclohexene, 3,3-dimethyl-1-(trimethylsilyloxy)-	13.470
71	D-(-)-Tagatofuranose, pentakis(trimethylsilyl) ether (isomer 1)	29.485
72	D-(-)-Tagatofuranose, pentakis(trimethylsilyl) ether (isomer 2)	29.112
73	Ethyl (trimethylsilyl)acetate	26.326
74	Ethyl linoleate 9,12-Octadecadienoic acid (9Z,12Z)-, ethyl ester	35.682
75	Ethyltriethylene glycol, TBDMS derivative	8.571
76	Glucitol, 6-O-nonyl-	20.304
77	Glutamic acid	19.734
78	Glycerol, 1-tert-butyl 3-trimethylsilyl ether	27.439
79	Hexadecanoic acid, 2,3-bis((trimethylsilyl)oxy)propyl ester (CAS)	43.160
80	Hexadecanoic acid, ethyl ester	32.433
81	Hexadecanoic acid, trimethylsilyl ester	33.509
82	Homovanillyl alcohol	37.871
83	Levoglucosan, 3TMS derivative	31.747
84	L-Glutamic acid	19.734
85	Linoelaidic acid	35.141
86	Linoelaidic acid, trimethylsilyl ester	36.642
87	Methyl .alpha.-D-glucofuranoside, 4TMS derivative	31.277
88	Myristic acid, TMS derivative	29.906
89	N-Hydroxymethyl fluoroacetamide	6.286

90	N-Methoxy-N-methylacetamide	5.819
91	N-Trifluoroacetyl-3-methoxytyramine, 2TMS derivative	39.029
92	Octadecanoic acid, ethyl ester	36.264
93	Octadecanoic acid, trimethylsilyl ester	37.195
94	Octane, 1-(1-ethoxyethoxy)-	20.304
95	Palmitate <ethyl-> Hexadecanoic acid, ethyl ester	32.433
96	Palmitic Acid, TMS derivative	33.509
97	Pentadecanoic acid, ethyl ester	32.433
98	Pentadecanoic acid, TMS derivative	31.277
99	Phloroglucinol, trimethylsilyl ether	13.470
100	Pidolic Acid	19.734
101	Pyrimidin-4(3H)-one, 2-amino-6-hydroxy-5-nitro-	6.286
102	Stearate <ethyl-> Octadecanoic acid, ethyl ester	36.264
103	Stearic acid, TMS derivative	37.195
104	Stigmast-5-en-3-ol	54.357
105	Stigmast-5-ene, 3.beta.-(trimethylsiloxy)-, (24S)-	54.886
106	Stigmasta-5,22-dien-3-ol, (3.beta.,22E)-	53.246
107	Stigmasterol	53.246
108	Tetradecanoic acid, trimethylsilyl ester	30.007
109	Trimethylsilyl 24-(trimethylsilyloxy)tetracosanoate)	31.747

The chemicals in the ethanol extract of the *Zingiber officinale* plant were interacted with the proteins of the SARS-CoV-2 virus, respectively. Molecular docking results obtained are given in Table 2. In this table, it can be seen that many parameters are calculated, the numerical values of which are sufficient data to compare the potential of molecules to inhibit the omicron variant of SARS-CoV-2 virus.

The chemicals in the ethanol extract of the *Zingiber officinale* plant were interacted with the proteins of the SARS-CoV-2 virus, respectively. Molecular docking results obtained are given in Table 2. In this table, it can be seen that many parameters are calculated, the numerical values of which are sufficient data to compare the potential of molecules to inhibit the omicron variant of SARS-CoV-2 virus.

**Table 2.** Numerical values of the docking parameters of molecule against SARS-CoV-2 virus

7QO7	Docking Score	Glide ligand efficiency	Glide hbond	Glide evdw	Glide ecoul	Glide emodel	Glide energy	Glide einternal	Glide posenum
Pyrimidin-4(3H)-one, 2-amino-6-hydroxy-5-nitro-1-(2,4-Dihydroxyphenyl)-2-(4-methoxy-3-nitrophenyl)ethanon	-5.78	-0.48	-0.48	-14.76	-10.10	-34.57	-24.86	0.21	77
e									
2,5-Monomethylene-rhamnitol	-5.33	-0.44	-0.32	-8.11	-16.22	-31.00	-24.33	2.03	95
Pidolic Acid	-5.21	-0.58	-0.70	-9.45	-8.22	-25.33	-17.67	0.81	233
2,3-Dihydro-3,5-dihydroxy-6-methyl-4H-pyran-4-one	-5.10	-0.51	-0.48	-13.79	-7.04	-30.15	-20.83	0.03	174

1,5-Anhydro-d-mannitol	-5.02	-0.46	0.00	-6.91	-15.60	-26.85	-22.51	3.87	203
Homovanillyl alcohol	-4.91	-0.41	-0.57	-15.37	-9.67	-31.39	-25.04	1.51	134
Phloroglucinol	-4.82	-0.37	-0.53	-14.42	-6.97	-28.35	-21.39	0.72	356
1-(3,4-Dimethoxyphenyl)decane-3,5-diyl diacetate	-4.82	-0.17	-0.05	-28.88	-5.00	-40.10	-33.88	8.01	187
1,4-Dioxan-2-ol, TMS derivative	-4.75	-0.43	-0.16	-17.27	-2.06	-24.63	-19.33	0.36	163
<b>7WRV</b>	<b>Docking Score</b>	<b>Glide ligand efficiency</b>	<b>Glide hbond</b>	<b>Glide evdw</b>	<b>Glide ecoul</b>	<b>Glide emodel</b>	<b>Glide energy</b>	<b>Glide einternal</b>	<b>Glide posenum</b>
2,5-Monomethylene-l-rhamnitol	-6.15	-0.51	-0.16	0.10	-27.31	-34.18	-27.20	4.26	359
Phloroglucinol, trimethylsilyl ether	-6.14	-0.47	-1.24	-17.05	-9.82	-35.06	-26.87	2.95	385
1,5-Anhydro-d-mannitol	-5.99	-0.54	-0.29	-3.34	-22.57	-32.54	-25.91	7.18	99
Pidolic Acid	-5.73	-0.64	-0.71	-11.27	-7.90	-30.43	-19.16	0.76	134
Pyrimidin-4(3H)-one, 2-amino-6-hydroxy-5-nitro-	-5.20	-0.43	-0.54	-13.47	-8.08	-31.42	-21.54	0.06	132
Glucitol, 6-O-nonyl-	-5.07	-0.24	-0.51	-20.45	-24.00	-54.82	-44.45	8.70	354
1,4-Dioxan-2-ol, TMS derivative	-5.04	-0.46	-0.42	-18.73	-5.98	-32.28	-24.71	0.34	108
3-Methoxy-N-(trifluoroacetyl)-O-(trimethylsilyl)tyrosine, trimethylsilyl ester	-5.01	-0.17	-0.61	-36.44	-7.34	-52.85	-43.78	9.47	5
1-(2,4-Dihydroxyphenyl)-2-(4-methoxy-3-nitrophenyl) ethanone	-4.99	-0.23	-0.89	-25.23	-9.46	-46.93	-34.69	4.50	240
2,3-Dihydro-Benzofuran	-4.79	-0.48	-0.04	-16.16	-2.56	-24.09	-18.72	0.00	271
<b>7U0N</b>	<b>Docking Score</b>	<b>Glide ligand efficiency</b>	<b>Glide hbond</b>	<b>Glide evdw</b>	<b>Glide ecoul</b>	<b>Glide emodel</b>	<b>Glide energy</b>	<b>Glide einternal</b>	<b>Glide posenum</b>
2,5-Monomethylene-l-rhamnitol	-6.74	-0.56	-0.32	-9.48	-21.83	-42.18	-31.31	3.13	162
2,2'-Ureylenebis(ethyl 3,3,3-trifluorolactate)	-6.45	-0.25	-0.90	-28.88	-20.73	-61.17	-49.61	11.19	93
1,5-Anhydro-d-mannitol	-6.22	-0.57	-0.05	-12.70	-15.06	-35.21	-27.76	5.12	99

2,3-Dimethyl-3-pentanol, TMS derivative	-5.65	-0.71	-0.32	-12.35	-6.82	-25.18	-19.17	0.76	264
Pyrimidin-4(3H)-one, 2-amino-6-hydroxy-5-nitro-1-(4-Hydroxy-3-methoxyphenyl)octane-3,5-diyl diacetate	-5.56	-0.46	-0.55	-20.09	-5.69	-34.74	-25.78	0.02	177
Pidolic Acid	-5.55	-0.22	-0.30	-35.36	-6.17	-50.17	-41.52	10.70	390
2,3-Dihydro-Benzofuran	-5.43	-0.60	-0.32	-18.28	-3.02	-28.93	-21.30	0.66	356
Homovanillyl alcohol	-5.38	-0.54	0.00	-19.95	-1.92	-28.69	-21.87	0.00	227
1,4-Dioxan-2-ol, TMS derivative	-5.35	-0.45	-0.14	-21.97	-5.97	-35.52	-27.93	2.18	177
	-5.33	-0.48	-0.52	-16.78	-5.13	-28.03	-21.91	0.45	250

In this study, SARS-CoV-2 virus has 4 different receptor sites. These four receptor sites are listed as follows; the spike (S) protein, nucleocapsid (N) protein, membrane (M) protein, and envelope (E) protein [26,27]. By targeting these receptor sites, it is aimed to inhibit the SARS-CoV-2 virus. Many variants of the SARS-CoV-2 virus are seen around the world. of these variants, BA.2.75 of the omicron variant of the SARS-CoV-2 virus, which is the fastest to meet and the last. This variant was targeted in this study.

However, the chemical found in the extract of the Zingiber officinale plant was detected individually

by GC-MS. The activities of each detected chemical molecule against the omicron variant of SARS-CoV-2 virus were compared. As a result of this comparison, 102 molecules interacted with the 7QO7 protein out of 109 molecules detected. 90 molecules interacted with the 7U0N protein. It was observed that 99 molecules interacted with the 7WRV protein. When it is desired to compare these interactions, the numerical value of the docking score parameter obtained from the molecular docking calculations of 109 molecules studied is examined.

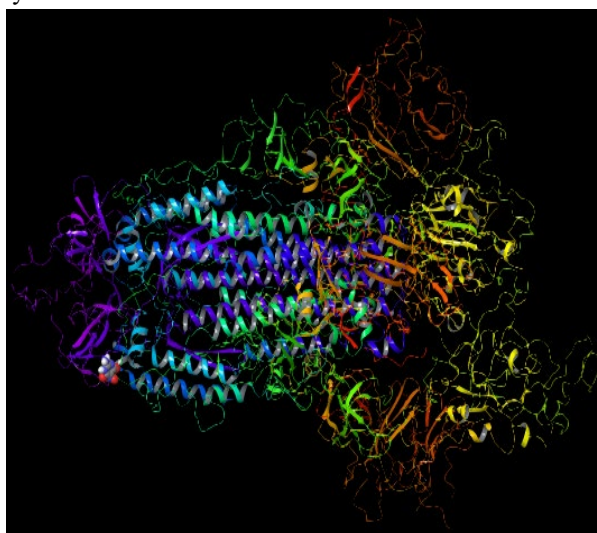
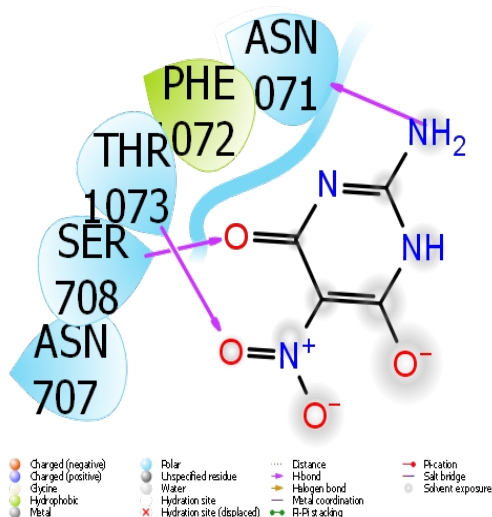


**Figure 2.** Presentation interactions of Pyrimidin-4(3H)-one, 2-amino-6-hydroxy-5-nitro- with 7QO7 protein

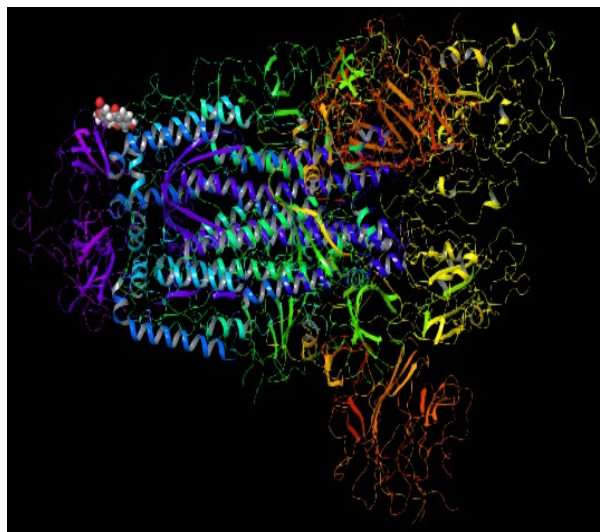
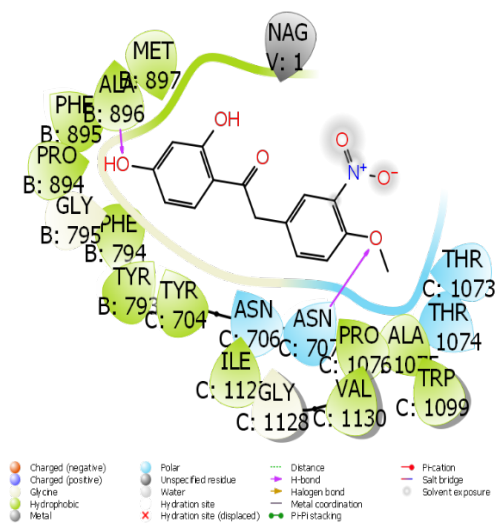


**Figure 3.** Presentation interactions of 1-(2,4-Dihydroxyphenyl)-2-(4-methoxy-3-nitrophenyl)ethanone with 7QO7

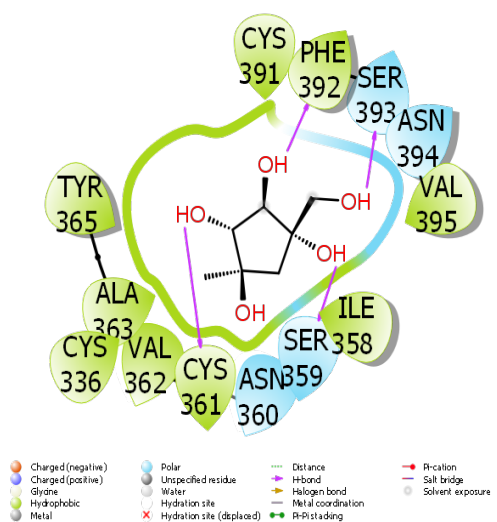


**Figure 4.** Presentation interactions of 2,5-Monomethylene-l-rhamnitol with 7WRV

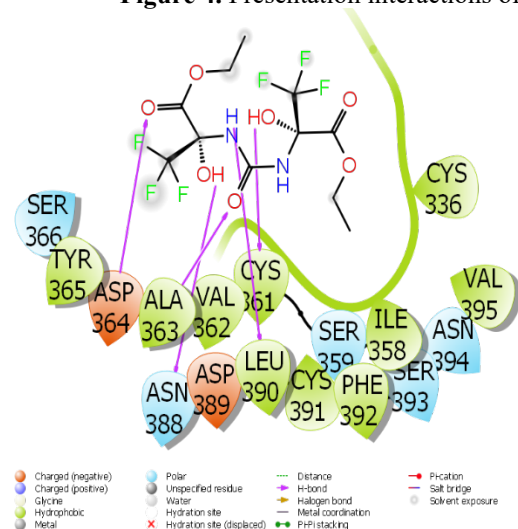


**Figure 5.** Presentation interactions of Phloroglucinol, trimethylsilyl ether with 7WRV

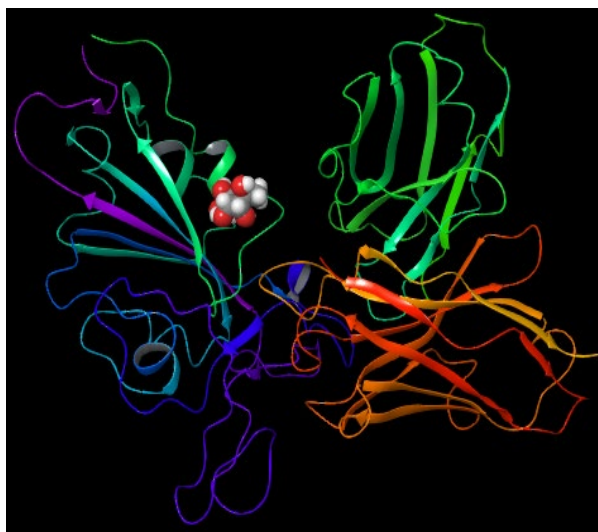
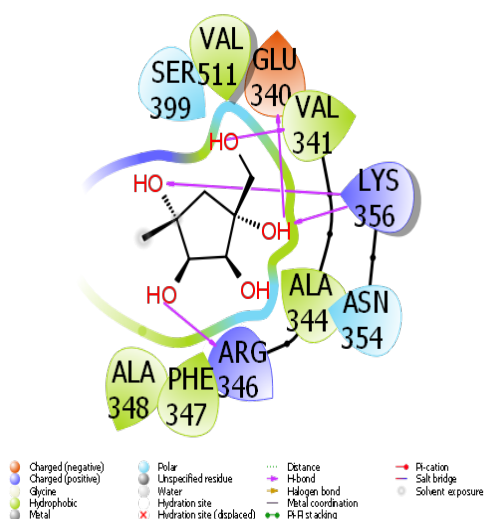


Figure 6. Presentation interactions of 2,5-Monomethylene-l-rhamnitol with 7U0N

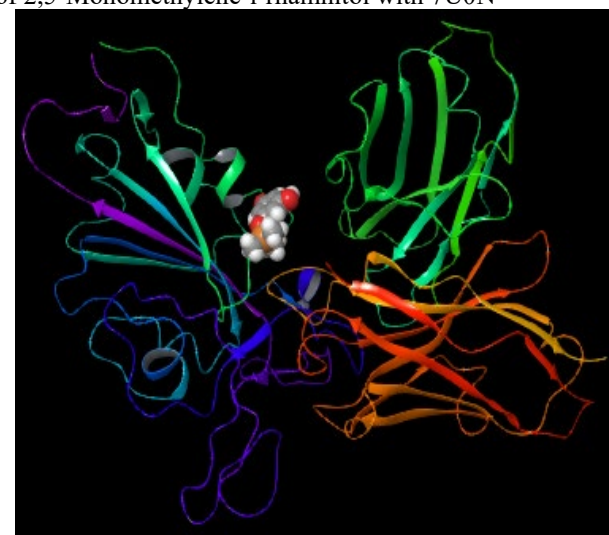
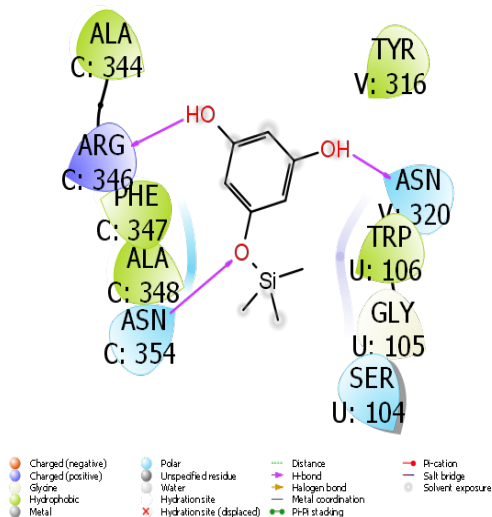


Figure 7. Presentation interactions of Ureylenebis(ethyl 3,3,3- with 7U0N

The interactions of molecules with omicron variants of SARS-CoV-2 are given in Figure 2-7. When the interaction of Pyrimidin-4(3H)-one, 2-amino-6-hydroxy-5-nitro- and 7QO7 protein in Figure 2 is examined, it is seen that the oxygen atom attached to the carbonyl carbon in this molecule forms a hydrogen bond interaction with the SER 378 protein. It is seen that the oxygen atom in the nitro group in the same molecule forms a hydrogen bond interaction with the THR 1073 protein. It is seen that the amino group attached to the central ring in the same molecule forms hydrogen bonds with the ASN 1071 protein. Figure 3 shows that the 1-(2,4-Dihydroxyphenyl)-2-(4-methoxy-3-nitrophenyl)ethanone molecule interacts with the 7QO7 protein, and the hydroxyl group in the phenol ring in this molecule forms hydrogen bonds with the ALA 896 protein. It is seen that the oxygen atom

in the ring attached to the nitro group in the same molecule makes hydrogen bonds with the ASN 707 protein. In Figure 4, in the interaction between the 2,5-Monomethylene-l-rhamnitol molecule and the 7WRV protein, it is seen that 4 of the 5 hydroxyl groups in the molecule form hydrogen bond interactions with the proteins CYS 361, SER 359, SER 393, and PHE 392, respectively. In Figure 5, it is seen that in the interaction between Phloroglucinol, trimethylsilyl ether and 7WRV protein, the oxygen atoms attached to the carbon of the two carbons in the molecule form a hydrogen bond interaction with ASP 364 and ALA 363 proteins. Two hydroxyl groups linked in the same molecule appear to form hydrogen bond interactions with ASN 388 and CYS 361 proteins, respectively. In Figure 6, it is seen that in the interaction between the 2,5-Monomethylene-l-

rhamnitol molecule and the 7U0N protein, 4 of the 5 hydroxyl groups in the molecule form hydrogen bond interactions with the proteins ARG 346, LYS 356, VAL 341, and GLU 341, respectively. In Figure 7, in the interaction between the Ureylenebis(ethyl 3,3,3- molecule and the 7U0N protein, it is seen that the two hydroxy groups in the molecule form a hydrogen bond interaction with the proteins ARG 346 and ASN 320. There is a hydrogen bonding interaction between the oxygen atom attached to the silicon atom in the same molecule and the ASN 354 protein.

It is not enough to compare the activities of molecules against SARS-CoV-2 virus and to use molecules as drugs. Because human metabolism

has a very complex structure. In order for molecules to be used as drugs, ADME/T calculations of molecules must be made. All parameters obtained as a result of these calculations are given in Table 3, which is examined and the possibility of being a drug is evaluated.

The numerical values of ADME/T parameters were calculated. It is possible to divide the calculated parameters into two groups. In the first group, the chemical properties of the molecules were investigated. for example, the molar mass of the molecules, the dipole moment, the Total solvent accessible surface area value, the volume of the molecules, and finally the number of hydrogen bonds taken and given by the molecule [28].

Table 3. Parameters of ADME/T analyze of molecules

Parameters	1	2	3	4	5	Reference Range
mol_MW	178	400	198	164	172	130-725
dipole (D)	1.9	6.1	4.0	6.5	15.7	1.0-12.5
SASA	359	607	443	342	321	300-1000
FOSA	165	263	228	166	0	0-750
FISA	194	150	109	176	293	7-330
PISA	0	0	107	0	28	0-450
WPSA	0	194	0	0	0	0-175
volume (A <sup>3</sup> )	578	1030	719	539	484	500-2000
donorHB	5	0.5	2	4	4	0-6
acptHB	6.6	2.5	2.35	8.5	5	2.0-20.0
glob (Sphere =1)	0.9	0.8	0.9	0.9	0.9	0.75-0.95
QPpolrz (A <sup>3</sup> )	13.1	29.9	21.1	12.2	11.6	13.0-70.0
QPlogPC16	6.4	7.6	6.8	5.6	6.0	4.0-18.0
QPlogPoct	14.7	12.7	10.8	14.9	19.4	8.0-35.0
QPlogPw	14.4	4.2	6.6	14.9	12.8	4.0-45.0
QPlogPo/w	-1.2	3.9	2.0	-1.5	-1.8	-2.0-6.5
QPlogS	-0.7	-5.8	-2.7	-0.8	-0.7	-6.5-0.5
CIQPlogS	-0.8	-5.8	-2.6	-0.4	-1.4	-6.5-0.5
QPlogHERG	-2.6	-3.2	-4.1	-2.6	-2.8	*
QPPCaco (nm/sec)	142	334	925	210	16	**
QPlogBB	-1.3	-1.0	-0.6	-1.1	-1.9	-3.0-1.2
QPPMDCK (nm/sec)	60	1976	455	92	6	**
QPlogKp	-4.5	-3.5	-2.8	-4.3	-6.5	***
IP (ev)	10.8	11.2	8.7	10.9	10.1	7.9-10.5
EA (eV)	-2.5	0.7	-0.6	-2.2	1.3	-0.9-1.7
#metab	5	2	2	5	2	1-8
QPlogKhsa	-0.9	0.3	-0.1	-0.9	-0.8	-1.5-1.5
Human Oral Absorption	2	3	3	2	2	-
Percent Human Oral Absorption	59	95	92	59	38	****
PSA	101	133	51	94	140	7-200
RuleOfFive	0	0	0	0	0	Maximum is 4
RuleOfThree	0	1	0	0	1	Maximum is 3

Jm 1.1 0.0 0.7 1.3 0.0 -

\* concern below -5, \*\*<25 is poor and >500 is great, \*\*\* K<sub>p</sub> in cm/hr,\*\*\*\* <25% is poor and >80% is high.

\*\*\*\*\*2,5-Monomethylene-1-rhamnitol is 1, 2,2'-Ureylenebis(ethyl 3,3,3-trifluorolactate) is 2, Phloroglucinol, trimethylsilyl ether is 3, 1,5-Anhydro-d-mannitol is 4, Pyrimidin-4(3H)-one, 2-amino-6-hydroxy-5-nitro- is 5

In the second part of the ADME/T calculations, the biological properties of the molecules were examined. These biological properties, the numerical value that predicts the passage of molecules through the blood-brain barrier and blood-intestinal barriers, the number of metabolic reactions, the permeability of the molecule when applied to human skin, the theoretically calculated qualitative human oral absorption amount, and finally the RuleOfFive, that is violations of Lipinski's rule of five, and RuleOfThree, that is violations of Jorgensen's rule of three, values of the molecules were calculated [29,30].

After molecular docking, ADME/T analysis was performed and many parameters were obtained from these calculations. Among these parameters, the numerical values of the calculated parameters such as QPPCaco (nm/sec) and QPPMDCK

(nm/sec) parameters seem to be quite low for crossing blood barriers. conversely, RuleOfFive and RuleOfThree provide important information about the conditions for being a drug.

It is seen that the molecules are in the desired range, whether they have chemical parameters or biological parameters. It is possible for each parameter molecule to be used as a drug in human metabolism. Since it is not possible to give all molecules in Table 3 in ADME/T calculations, molecular docking calculations have given the molecules with the highest activity in all SARS-CoV-2 proteins. The calculations made must be compared with FDA (U.S. Food and Drug Administration) approved drugs in order for the results to be meaningful. The results of the calculations for this are given in Table 4.

**Table 4.** Numerical values of the docking parameters of molecule against SARS-CoV-2 virus

7QO7	Docking Score	Glide ligand efficiency	Glide hbond	Glide evdw	Glide ecoul	Glide emodel	Glide energy	Glide einternal	Glide posenum
121304016	-5.74	-0.14	-0.52	-37.03	-11.46	-57.49	-48.49	12.47	90
492405	-5.56	-0.51	-0.61	-13.92	-7.96	-29.02	-21.88	1.77	258
131411	-3.53	-0.12	0.00	-31.83	-3.10	-40.86	-34.94	3.66	261
84029	-2.91	-0.06	0.00	-19.91	-8.64	-26.61	-28.55	8.33	289
7WRV	Docking Score	Glide ligand efficiency	Glide hbond	Glide evdw	Glide ecoul	Glide emodel	Glide energy	Glide einternal	Glide posenum
121304016	-6.09	-0.15	-1.03	-37.27	-16.30	-69.64	-53.57	7.43	284
92727	-5.74	-0.12	-0.55	-43.55	-8.35	-65.23	-51.90	9.63	374
492405	-5.25	-0.48	-0.61	-15.86	-6.68	-31.39	-22.54	2.07	42
84029	-3.69	-0.07	-0.16	-16.87	-13.01	-22.68	-29.88	36.35	395
131411	-3.68	-0.13	-0.16	-32.40	-7.22	-46.56	-39.62	5.94	126
7U0N	Docking Score	Glide ligand efficiency	Glide hbond	Glide evdw	Glide ecoul	Glide emodel	Glide energy	Glide einternal	Glide posenum
121304016	-6.51	-0.16	-0.58	-44.96	-10.66	-70.70	-55.62	12.82	156
492405	-5.92	-0.54	-0.81	-18.08	-7.90	-34.06	-25.98	1.97	225
131411	-3.90	-0.13	-0.28	-36.33	-8.13	-56.42	-44.46	2.78	260
84029	-3.13	-0.06	-0.02	-25.29	-7.23	-32.87	-32.53	13.63	114

In light of the explanations made above, comparison of molecules with FDA-approved drugs is too important to recommend molecules as drugs. FDA-approved drugs used are commonly used drugs such as Favipiravir (PubChem CID: 492405), Arbidol (PubChem CID: 131411), Remdesivir (PubChem CID: 121304016), Clarithromycin (PubChem CID: 84029), and Lopinavir (PubChem CID: 92727) used for comparison as reference molecules.

As a result of the calculations, it was seen that Pyrimidin-4(3H)-one, 2-amino-6-hydroxy-5-nitro-molecule had higher activity against 7QO7 protein with a docking score parameter value of -5.78. On the other hand, 2,5-Monomethylene-l-rhamnitol molecule was found to have higher activity than other molecules with a docking score of -6.15. Finally, 2,5-Monomethylene-l-rhamnitol molecule was found to have higher activity than other molecules with a docking score of -6.74. Compared with FDA-approved drugs, the molecules studied had higher activity than FDA-approved drugs.

#### 4. Conclusions

As a result of theoretical calculations, Zingiber officinale plant was found to contain many chemicals as a result of GC-MS analysis. These chemicals were detected one by one and their activity values were calculated for the SARS-CoV-2 virus. As a result, molecules with high activity were detected. ADME/T properties were investigated in order to examine the drug properties of molecules with high activity. According to ADME/T results, these five molecules examined are suitable for use in human metabolism as drug molecules. The theoretical results here will be an important guide for future in vitro and in vivo studies.

#### ACKNOWLEDGEMENT

The numerical calculations reported in this paper were fully/partially performed at TUBITAK ULAKBIM, High Performance and Grid Computing Center (TRUBA resources). This work was supported by the Scientific Research Project Fund of Sivas Cumhuriyet University (CUBAP) under the project number RGD-020.

#### References

[1] M. Boozari, H. Hosseinzadeh, Natural products for COVID-19 prevention and treatment regarding

to previous coronavirus infections and novel studies. *Phytotherapy Research*, 35(2) (2021) 864-876.

- [2] N. Gangal, V. Nagle, Y. Pawar, S. Dasgupta, Reconsidering traditional medicinal plants to combat COVID-19. *AIJR Preprints*, 34 (2020) 1-6.
- [3] J.N.M. Kanyinda, Coronavirus (COVID-19): a protocol for prevention and treatment (Covalyse®). *European Journal of Medical and Health Sciences*, (2020) 2(3).
- [4] M. Mesri, S.S.E. Saber, M. Godazi, A.R. Shirdel, R. Montazer, H.R., Koohestani, ... & N. Azizi, The effects of combination of Zingiber officinale and Echinacea on alleviation of clinical symptoms and hospitalization rate of suspected COVID-19 outpatients: a randomized controlled trial. *Journal of Complementary and Integrative Medicine*, 18(4) (2021) 775-781.
- [5] D. S. N. B. K. Prasanth, M. Murahari, V. Chandramohan, G. Bhavya, A. Lakshmana Rao, S.P. Panda, ... T. Jaswitha, In-silico strategies of some selected phytoconstituents from *Melissa officinalis* as SARS CoV-2 main protease and spike protein (COVID-19) inhibitors. *Molecular Simulation*, 47(6) (2021) 457-470.
- [6] S. Banerjee, H.I. Mullick, J. Banerjee, A. Ghosh, Zingiber officinale: 'a natural gold'. *Int J Pharmaceutical Bio-Sci*, 2 (2011) 283-94.
- [7] K. Ghafoor, F. Al Juhaimi, M.M. Özcan, N. Uslu, E.E. Babiker, I.A.M. Ahmed, Total phenolics, total carotenoids, individual phenolics and antioxidant activity of ginger

- (Zingiber officinale) rhizome as affected by drying methods. *Lwt*, 126 (2020) 109354.
- [8] A. M. A. Ali, M. E. M. El-Nour, S. M. Yagi, Total phenolic and flavonoid contents and antioxidant activity of ginger (*Zingiber officinale* Rosc.) rhizome, callus and callus treated with some elicitors. *Journal of genetic engineering and biotechnology*, 16(2) (2018) 677-682.
- [9] Q. Q. Mao, X. Y. Xu, S. Y. Cao, R. Y. Gan, H. Corke, T. Beta, H. B. Li, Bioactive compounds and bioactivities of ginger (*Zingiber officinale* Roscoe). *Foods*, 8(6) (2019) 185.
- [10] M. H. Shahrajabian, W. Sun, Q. Cheng, Clinical aspects and health benefits of ginger (*Zingiber officinale*) in both traditional Chinese medicine and modern industry. *Acta agriculturae scandinavica, section b—Soil & Plant Science*, 69(6) (2019) 546-556.
- [11] A. P. Shirin, P. Jamuna, Chemical composition and antioxidant properties of ginger root (*Zingiber officinale*). *Journal of Medicinal Plants Research*, 4(24) (2010) 2674-2679.
- [12] M. Haridas, V. Sasidhar, P. Nath, J. Abhithaj, A. Sabu, P. Rammanohar, Compounds of *Citrus medica* and *Zingiber officinale* for COVID-19 inhibition: in silico evidence for cues from Ayurveda. *Future journal of pharmaceutical sciences*, 7(1) (2021) 1-9.
- [13] I. Kravchenko, L. Eberle, M. Nesterkina, A. Kobernik, Anti-inflammatory and analgesic activity of ointment based on dense ginger extract (*Zingiber officinale*). *Journal of Herbmед Pharmacology*, 8(2) (2019) 126-132.
- [14] A. Poustforoosh, H. Hashemipour, B. Tüzün, M. Azadpour, S. Faramarz, A. Pardakhty, ... & M.H. Nematollahi, The Impact of D614G Mutation of SARS-COV-2 on the Efficacy of Anti-viral Drugs: A Comparative Molecular Docking and Molecular Dynamics Study. *Current microbiology*, 79(8) (2022) 1-12.
- [15] B. Tüzün, K. Sayin, H. Ataseven, Could *Momordica Charantia* Be Effective In The Treatment of COVID19?. *Cumhuriyet Science Journal*, 43(2) (2022) 211-220.
- [16] H. Karataş, B. Tüzün, Z. Kökbudak, Could pyrimidine derivative be effective against Omicron of SARS-CoV-2?. *Bratislava Medical Journal- Bratislavske Lekarske Listy*, 123(7) (2022) 505-513.
- [17] A. Aktaş, B. Tüzün, R. Aslan, K. Sayin, H. Ataseven, New anti-viral drugs for the treatment of COVID-19 instead of favipiravir. *Journal of Biomolecular Structure and Dynamics*, 39(18) (2021) 7263-7273.
- [18] D. Ni, K. Lau, P. Turelli, C. Raclot, B. Beckert, S. Nazarov, ... & D. Trono, Structural analysis of the Spike of the Omicron SARS-COV-2 variant by cryo-EM and implications for immune evasion. *bioRxiv* (2021).
- [19] Q. Geng, K. Shi, G. Ye, W. Zhang, H. Aihara, F. Li, Structural Basis for Human Receptor Recognition by SARS-CoV-2 Omicron Variant BA. 1. *Journal of Virology*, 96(8) (2022) e00249-22.
- [20] W. Yin, Y. Xu, P. Xu, X. Cao, C. Wu, C. Gu, ... & H. E. Xu, Structures

- of the Omicron Spike trimer with ACE2 and an anti-Omicron antibody. *Science*, 375(6584) (2022) 1048-1053.
- [21] Schrödinger Release 2021-3: Maestro, Schrödinger, LLC, New York, NY, 2021.
- [22] Schrödinger Release 2019-4: Protein Preparation Wizard; Epik, Schrödinger, LLC, New York, NY, 2016; Impact, Schrödinger, LLC, New York, NY, 2016; Prime, Schrödinger, LLC, New York, NY, 2019.
- [23] Schrödinger Release 2021-3: LigPrep, Schrödinger, LLC, New York, NY, 2021.
- [24] A. Poustforoosh, H. Hashemipour, B. Tüzün, A. Pardakhty, M. Mehrabani, & M. H. Nematollahi, Evaluation of potential anti-RNA-dependent RNA polymerase (RdRP) drugs against the newly emerged model of COVID-19 RdRP using computational methods. *Biophysical chemistry*, 272 (2021) 106564.
- [25] Schrödinger Release 2021-3: QikProp, Schrödinger, LLC, New York, NY, 2021.
- [26] H. Kekeçmuhammed, M. Tapera, B. Tüzün, S. Akkoç, Y. Zorlu, E. Sarıpınar, Synthesis, Molecular Docking and Antiproliferative Activity Studies of a Thiazole-Based Compound Linked to Hydrazone Moiety. *ChemistrySelect*, 7(26) (2022) e202201502.
- [27] M. Tapera, H. Kekeçmuhammed, B. Tüzün, E. Sarıpınar, Ü. M. Koçyiğit, E. Yıldırım, ... & Y. Zorlu, Synthesis, carbonic anhydrase inhibitory activity, anticancer activity and molecular docking studies of new imidazolyl hydrazone derivatives. *Journal of Molecular Structure*, 1269 (2022) 133816.
- [28] A. Mermer, M. V. Bulbul, S. M. Kalender, I. Keskin, B. Tuzun, O. E. Eyupoglu, Benzotriazole-oxadiazole hybrid Compounds: Synthesis, anticancer Activity, molecular docking and ADME profiling studies. *Journal of Molecular Liquids*, 359 (2022) 119264.
- [29] H. Yalazan, B. Tüzün, D. Akkaya, B. Barut, H. Kantekin, S. Yıldırım, Quinoline-fused both non-peripheral and peripheral ZnII and MgII phthalocyanines: Anti-cholinesterase, anti- $\alpha$ -glucosidase, DNA nuclease, antioxidant activities, and in silico studies. *Applied Organometallic Chemistry*, (2022) e6696.
- [30] M. S. Çelik, Ş. A. Çetinus, A. F. Yenidünya, S. Çetinkaya, B. Tüzün, Biosorption of Rhodamine B dye from aqueous solution by *Rhus coriaria* L. plant: Equilibrium, kinetic, thermodynamic and DFT calculations. *Journal of Molecular Structure*, 1272 (2023) 134158.